

ACTIVE MEDIA

PACS numbers: 42.70.Hj; 42.70.Ce; 42.55.Rz; 42.60.Lh
DOI: 10.1070/QE2009v039n12ABEH014193

New high-strength neodymium phosphate laser glass

B.I. Galagan, I.N. Glushchenko, B.I. Denker, Yu.L. Kalachev,
N.V. Kuleshov, V.A. Mikhailov, S.E. Sverchkov, I.A. Shcherbakov

***Abstract*. A high-strength neodymium laser glass (SNLG) based on an alumoborophosphate composition is developed and synthesised; its physicochemical, spectral, luminescent, and lasing characteristics are studied. It is found that the chemical stability and thermal resistance of the new glass are considerably higher than the corresponding characteristics of known neodymium-doped phosphate laser glasses. Investigations of lasing upon longitudinal diode pumping showed that, due to the higher thermal resistance, the new glass allows one to obtain output powers twice as high as those of industrial GLS22 glass.**

Keywords: *laser glass, neodymium, diode pumping*

1. Introduction

Neodymium-glass lasers take an important place in quantum electronics. These lasers operate in various regimes, from femtosecond pulses to cw lasing. The most widespread are neodymium laser glasses based on phosphorus or silicon oxides as glass-forming materials. The main advantages of neodymium phosphate glasses compared to silicate glasses are the large cross section of the fundamental laser transition (in the region of 1.06 μm) and the possibility of lasing on the transition in the region of 1.3 μm. The drawbacks of phosphate glasses are that they have a lower mechanical strength than silicate glasses, which does not allow one to use high average pump powers, and a low resistance to atmospheric moisture. These drawbacks are caused by low chemical bonds between the main structural elements of phosphate glasses (PO_4 tetrahedrons) [1].

The aim of this work is to develop and study a neodymium-doped glass that combines the excellent spectral and luminescent properties of phosphate glasses with high thermomechanical strength and chemical stability. Note that we previously solved a similar problem was for ytterbium–erbium and ytterbium laser glasses [2, 3]. In these works, we increased the glass strength by introducting significant amounts of boron and aluminium oxides into the glass composition, thus forming in the glass a strong three-dimensional structure of alternating PO_4, BO_4, and AlO_4 groups.

B.I. Galagan, I.N. Glushchenko, B.I. Denker, Yu.L. Kalachev, V.A. Mikhailov, S.E. Sverchkov, I.A. Shcherbakov A.M. Prokhorov General Physics Institute, Russian Academy of Sciences, ul. Vavilova 38, 119991 Moscow, Russia; e-mail: galagan@ran.gpi.ru, dikibill@mail.ru;
N.V. Kuleshov Institute of Optical Materials and Technologies, Belarussian National Technical University, prosp. Nezavisimosti 65, bldg. 17, 220013 Minsk, Belarus

Received 21 July 2009; revision received 15 October 2009
Kvantovaya Elektronika **39** (12) 1117 – 1120 (2009)
Translated by M.N. Basieva

2. Choice of the composition, glass synthesis, and preparation of samples for investigations

The new high-strength neodymium glass composition was searched for using the results of studies [2, 3]. The typical concentration of neodymium in laser glasses is $(1-4)\times 10^{20}$ cm^{-3}, which is approximately an order of magnitude lower than the total concentration of rare-earth ions in Yb – Er glass [2]. This allowed us, taking as a base the glass composition from [2], to increase the content of aluminium oxide by decreasing the concentration of rare-earth oxides, which, in turn, was expected to increase the chemical stability and strength of glass. The most important technological requirement for the choice of compositions was the crystallisation resistance that allowed synthesis of glass in volumes exceeding 1 L.

As a result, we chose the following molar composition of neodymium-doped alumoborophosphate laser glass: LiF (16 %), Al_2O_3 (12 %), B_2O_3 (13 %), P_2O_5 (57 %), and $La_2O_3 + Nd_2O_3$ (2 %). In this composition, lanthanum isomorphically substitutes neodymium in the glass matrix and thus makes it possible to vary the neodymium concentration.

For lasing and spectroscopic investigations, we prepared (in platinum crucibles with induction heating) two glass moulds 0.5 an 0.05 L in volume with different neodymium concentrations. In the first mould, the neodymium concentration was 2×10^{20} cm^{-3}, which corresponds to the conventional concentration of neodymium in laser materials. The smaller mould with the dopant concentration – 2×10^{19} cm^{-3} was used only for spectral-luminescent studies. Visual control showed neither gaseous nor crystalline inclusions in the main body of glasses. We also observed no refractive index inhomogeneities (streaks) and no strong light scattering. The absorption at the wavelength 3.33 μm was 3 – 4 cm^{-1}, which provides an estimate of the degree of dehydration of synthesised glasses. From the glass moulds, we prepared 1.5-mm-long polished plates 5 mm in diameter for spectral-luminescent studies, different samples for physicochemical tests, and 2.5-mm-long active elements 5 mm in diameter for lasing experiments.

3. Physicochemical properties and spectral-luminescent characteristics

Some parameters of the synthesised SNLG in comparison with well-known GLS22 (Russia) [4, 5] and QX/Nd (Kigre Inc., USA) [6, 7] neodymium-doped phosphate glasses are given below. These characteristics were determined by the methods described in [4–9]. The thermal shock resistance was estimated by the method of [7], according to which we heated the samples 5 mm in diameter and 15 mm long to a particular temperature, which was successively increased in each experiment, threw them in water (at room temperature), and measured the temperature difference at which the samples were destroyed. The thermal expansion coefficient α and the temperature coefficient of the refractive index dn/dT were determined by the interference method [8] in the temperature range of 30–70 °C.

The effective fluorescence bandwidth $\Delta\lambda_{\text{eff}}$ ($^4F_{3/2} - {}^4I_{11/2}$ transition) was found as the ratio of the area under the fluorescence curve to the maximum intensity with allowance for the quantum spectral sensitivity of the detector. The branching ratio β was determined as the ratio of the area under one of the three fluorescence bands to the sum of the areas of all the three bands. The $^4F_{3/2} - {}^4I_{11/2}$ laser transition cross section was calculated according to the method of [9] by the formula

$$\sigma = \frac{\lambda_{\max}^4 \beta}{8\pi c n^2 \tau_{\text{rad}} \Delta\lambda_{\text{eff}}},$$

where $\lambda_{\max}$ is the position of the fluorescence band peak and c is the velocity of light. As τ_{rad} in calculations of σ, we used the lifetime of the metastable state of neodymium in the sample with the low (2×10^{19} cm^{-3}) dopant concentration.

The presented characteristics show that the synthesised SNLG has a noticeably better chemical stability than the known laser glasses: its moisture resistance corresponds to the highest category A compared to the lowest category D of GLS22 and the weight loss in boiling water is fivefold lower than that for QX/Nd. The thermal shock resistance of SNLG is even twofold higher than of QX/Nd glass, which is one of the most thermally stable neodymium phosphate glasses. Our physicochemical investigations have shown that such SNLG properties as moisture resistance, hardness, thermal expansion coefficient, and thermal resistance lie in the region typical for much harder and chemically more stable silicate glasses. At the same time, its spectral-luminescent characteristics (the position of the fluorescence maximum, the metastable level lifetime, and the laser transition cross section) are highly competitive with the corresponding characteristics of the known neodymium-doped phosphate laser glasses. Thus, we can expect that the use of the synthesised glass will allow one to exceed the average output power of phosphate glass lasers.

4. Lasing investigations

The lasing characteristics of active elements (AEs) made of SNLG and GLS22 were studied under the maximally similar experimental conditions in order to correctly compare their lasing properties. The AEs have identical dimensions (5 mm in diameter and 2.5 mm long) and their faces were simultaneously mirror coated in one deposition process. The reflection coefficients of coatings of the output and input mirrors at the laser wavelength 1.06 μm were 97 % and 99.9 %, respectively. The input mirror had an AR coating for the pump wavelength (803.5 nm).

As a pump source, we used a LIMO fibre-coupled diode

	SNLG	GLS22	QX/Nd
Refractive index n	1.538 ± 0.002	1.596	1.538
Thermal expansion $\alpha/10^{-7}$ K^{-1}	66	102	72
$\frac{dn}{dT}/10^{-7}$ K^{-1}	58.5	−57	−4
Thermooptical coefficient $W = dn/dT + \alpha(n-1)/10^{-7}$ K^{-1}	94	4	51
Density at 20 °C/g cm^{-3}	2.83	3.52	2.66
Thermal conductivity/W m^{-1} K^{-1}	0.83 ± 0.04	0.395	0.85
Heat capacity/J cm^{-3} K^{-1}	2.06 ± 0.05	1.99	–
Knoop hardness/kgf mm^{-2}	712 ± 30	360	503
Weight loss in boiling water/10^{-5}g cm^{-2} h^{-1}	< 1	–	5
Acid resistance (GOST 13917-82) group	1	1	–
Moisture resistance (GOST 13917-82) group	A	D	–
Glass transition temperature/°C	600	510	506
Deformation temperature/°C	650	550	535
Thermal shock resistance/°C	165–175	35–38	80–95
Concentration of Nd^{3+} ions/10^{20} cm^{-3}	2	2	–
Fluorescence peak wavelength $\lambda_{\max}$ (transition $^4F_{3/2} - {}^4I_{11/2}$)/μm	1.055	1.055	1.054
Effective fluorescence bandwidth $\Delta\lambda_{\text{eff}}$ (transition $^4F_{3/2} - {}^4I_{11/2}$)/nm	27.7	28.6	27.6
Branching ratio β (%)			
transition $^4F_{3/2} - {}^4I_{11/2}$	50	51	–
transition $^4F_{3/2} - {}^4I_{9/2}$	43	41	–
transition $^4F_{3/2} - {}^4I_{13/2}$	7	8	–
$^4F_{3/2} - {}^4I_{11/2}$ laser transition cross section $\sigma/10^{-20}$ cm^2	3.2	3.2–3.6	3.34–3.8
Metastable state lifetime τ/μs	280 ± 4	250	–
Radiative lifetime of the metastable state τ_{rad}/μs	380 ± 4	350	353
Fluorescence quantum yield η	0.74	0.73–0.74	–

array with an output power up to 15 W. The quartz fibre core diameter and numerical aperture were 200 μm and 0.22. The pump radiation wavelength at the diode operating temperature of 23 °C was 803.5 nm with the spectral width ~ 7 nm. At these pump parameters, the pump radiation spectrum almost completely overlapped with the neodymium absorption band in the studied materials. The pump radiation was focused into the AE to a spot 150 μm in diameter.

The active element was sandwiched between indium foil gaskets and clamped between two heat-sink aluminium plates with apertures 1.5 mm in diameter. The cavity length was determined by the AE thickness. At such a short cavity, it was possible to achieve stable cw lasing in a rather large range of average pump powers despite significant pump-induced thermooptical distortions in the AE.

We achieved a cw output power up to 300 mW at a pump power of 3.2 W in the laser with the SNLG AE and an output power up to 160 mW at a pump power of 1.4 W in the GLS22 laser (Fig. 1). In the latter case, a further increase in the pump power lead to destruction of the AE (appearance of cracks) in the region of incidence of pump radiation. Lasing experiments were performed with three laser elements of each type up to their destruction. The characteristics of lasers with the SNLG and GLS22 AEs are given below. Thus, it is experimentally found that the AEs made of the new SNLG can operate without destruction at an approximately 2.2-fold higher pump power, which allows one to achieve a higher output power.

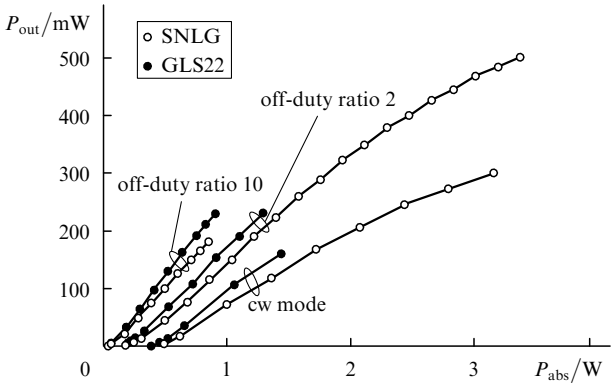

Figure 1. Average output powers of SNLG and GLS22 lasers as functions of the absorbed pump power.

	SNLG	GLS22
Absorbed part of the pump power (%)	68	72
Threshold pump power/mW	490	454
Maximum achieved output power/mW		
pulsed (with a pump pulse off-duty factor of 10)	1800	2290
average (with an off-duty factor of 2)	500	230
in a cw lasing regime	300	160
Slope efficiency (%)		
with an off-duty factor of 10	22	26.4
with an off-duty factor of 2	18	20.8
upon cw pumping	13.4	16.25
Beam divergence at the lasing threshold/mrad	13.4	13.4
Breakdown threshold pump power/W	3.2	1.4
Maximum of the emission spectrum/nm	1054	1056
Laser emission bandwidth/nm	7.5	7.5

In the case of pulse periodic pumping (with the pump pulse duration of 10 ms), the lasing efficiency considerably increased for both lasers due to a decrease in the thermal load on the AEs and, hence, to smaller thermooptical distortions in them and correspondingly smaller intracavity losses (see Fig.1). In particular, for the SNGL element, the slope efficiency at an off-duty ratio of 2 increased to 18 % at an average output power of ~ 500 mW, while the slope efficiency at an duty-off ratio of 10 was 22 % at a pulsed output power of 1.8 W.

Note that the efficiency of the GLS22 laser was somewhat higher than the efficiency of the laser with the SNGL AE (see Fig. 1). Comparison of the transmission spectra of these glasses showed that the absorption coefficient of SNGL (0.02 cm^{-1}) at the laser wavelength is noticeably higher than that of GLS22 (0.002 cm^{-1}). Obviously, this fact is responsible for the lower efficiency of the laser based on the new glass.

The laser beam divergence (Fig. 2) and spectral composition were measured in the cw lasing regime. Slightly above the pump threshold, both lasers generate single-mode radiation with almost the same divergence and an approximately Gaussian distribution. With increasing the average pump power, the lasers begin to operate in a multimode regime. In the region of pump powers close to the GLS22 breakdown threshold, the beam divergences almost coincide for both lasers. With increasing the pump power to 3 W, the output beam divergence for the SNGL laser increases to ~ 50 mrad. The laser wavelength was 1054 nm for SNGL and 1056 nm for GLS22. The emission bandwidth for the two lasers was ~ 7.5 nm both at the lasing threshold and at the maximum pump powers.

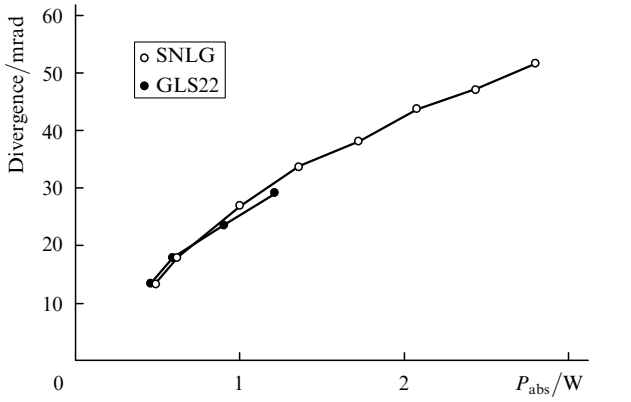

Figure 2. Dependences of the beam divergence on the absorbed pump power for lasers with SNLG and GLS22 AEs.

5. Conclusions

We have studied the physicochemical, spectral-luminescent, and lasing properties of a new neodymium laser glass based on an alumoborophosphate composition. Our investigations have shown that this glass has a high chemical stability and thermal resistance, which are more typical for silicate glasses. At the same time, its spectral-luminescent characteristics (the fluorescence maximum position, the metastable level lifetime, and the laser transition cross section) are highly competitive with the corresponding

characteristics of well-known neodymium-doped phosphate laser glasses. A 0.5-L mould of laser-quality glass doped with neodymium with a concentration of 2×10^{20} cm^{-3} is synthesised and used to prepare active elements. Lasing experiments upon longitudinal diode pumping have shown that the new material can withstand a 2.2-fold higher pump power than GLS22, which allowed us to obtain approximately twofold higher average output powers.

References

1. Alekseev N.E., Gapontsev V.P., Zhabotinskii M.E., Kravchenko V.B., Rudnitskii Yu.P. *Lazernye fosfatnye stekla* (Laser phosphate glasses) (Moscow: Nauka, 1980).
2. Karlsson G., Laurell F., Tellefsen J., Denker B., Galagan B., Osiko V., Sverchkov S. *Appl. Phys. B*, **75**, 41 (2002).
3. Galagan B.I., Glushchenko I.N., Denker B.I., Kisel' V.E., Kuril'chik S.V., Kuleshov N.V., Sverchkov S.E. *Kvantovaya Elektron.*, **39** (10) 891 (2009) [*Quantum Electron.*, **39** (10) 891 (2009)].
4. Prokhorov A.M. (Ed.) *Spravochnik po lazeram* (Laser Handbook) (Moscow: Sov. radio, 1978) Vol. 1.
5. Avakyants L.I., Buzhinskii I.M., Koryagina E.I., Surkova V.F. *Kvantovaya Elektron.*, **5** (4) 725 (1978) [*Sov. J. Quantum Electron.*, **8** (4), 423 (1978)].
6. www. kigre.com.
7. Jiang Sh., Myers J.D., Wu R., Bishop G.M., Rhonehouse D.L., Myers M.J., Hamlin S.J. *Proc. SPIE Int. Soc. Opt. Eng.*, **2379**, 17 (1995).
8. Sverchkov S.E. *Cand. Diss.* (Moscow: GPI RAS, 2005).
9. Dianov E.M., Karasik A.Ya., Kornienko L.S., Prokhorov A.M., Shcherbakov I.A. *Kvantovaya Elektron.*, **2** (8) 1665 (1975) [*Sov. J. Quantum Electron.*, **5** (8), 901 (1975)].